Diagn Interv Radiol 2021; 27:768–773

INTERVENTIONAL RADIOLOGY

ORIGINAL ARTICLE

Antireflux catheter improves tumor targeting in liver radioembolization with resin microspheres

Philippe d'Abadie
Stephan Walrand
Pierre Goffette
Nadia Amini
Aline van Maanen
Renaud Lhommel
François Jamar

PURPOSE
We aimed to determine whether antireflux (ARC) catheter may result in better tumor targeting in liver radioembolization using ^{90}Y-resin microspheres.

METHODS
Patients treated with resin microspheres for hepatocellular carcinoma (HCC) and secondary liver malignancies were retrospectively analyzed. All patients underwent a ^{99m}Tc-macroaggregated albumin (^{99m}Tc-MAA) single photon emission computed tomography (SPECT) following the planning arteriography with a conventional end-hole catheter. For ^{90}Y-microspheres injection, two groups were defined depending on the type of catheter used: an ARC group (n=38) and a control group treated with a conventional end-hole catheter (n=23). ^{90}Y positron emission tomography computed tomography (PET/CT) was performed after the therapeutic arteriography. The choice of the catheter was not randomized, but left to the choice of the interventional radiologist. ^{99m}Tc-MAA SPECT and ^{90}Y PET/CT were co-registered with the baseline imaging to determine a tumor to normal liver ratio ($T/NL_{[MAA\ or\ 90Y]}$) and tumor dose ($TD_{[MAA\ or\ 90Y]}$) for the planning and therapy.

RESULTS
Overall, 38 patients (115 lesions) and 23 patients (75 lesions) were analyzed in the ARC and control groups, respectively. In the ARC group, T/NL_{90Y} and TD_{90Y} were significantly higher than T/NL_{MAA} and TD_{MAA}. Median (IQR) T/NL_{90Y} was 2.16 (2.15) versus 1.74 (1.43) for T/NL_{MAA} ($p < 0.001$). Median (IQR) TD_{90Y} was 90.96 Gy (98.31 Gy) versus 73.72 Gy (63.82 Gy) for TD_{MAA} ($p < 0.001$). In this group, the differences were highly significant for neuroendocrine metastases (NEM) and HCC and less significant for colorectal metastases (CRM). In the control group, no significant differences were demonstrated.

CONCLUSION
The use of an ARC significantly improves tumor deposition in liver radioembolization with resin microspheres.

Yttrium-90 (^{90}Y) radioembolization is a locoregional therapy for hepatocellular carcinoma (HCC) and secondary liver malignancies. ^{90}Y-loaded microspheres are injected in the liver target volume (containing tumors) during arterial catheterization. This treatment aims at reaching an efficient absorbed dose to tumors while minimizing radiation dose to the healthy liver in order to prevent toxicity (1).

Before treatment, a planning arteriography is always performed for evaluating the feasibility of radioembolization. For this purpose, the treatment is simulated with intra-arterial injection of ^{99m}Tc-macroaggregated albumin (MAA) particles (2). Afterwards, ^{99}Tc-MAA nuclear imaging is performed to estimate lung shunt, for ruling out extrahepatic deposition and for dosimetry calculations (3, 4). Previous studies demonstrated a strong relationship between the tumor dose evaluated on ^{99m}Tc-MAA single photon emission computed tomography (SPECT) imaging and the tumor response, especially for HCC (3).

Better tumor targeting is a real challenge to improve clinical results of radioembolization. An increase in the tumor dose leads to an increase in the tumor control probability and in patient outcome (5). The technique has evolved recently, especially in the field of interventional radiology, for instance by the use of cone beam computed tomography (CT) for accurate planning or by using special microcatheters, such as antireflux catheters

From the Department of Nuclear Medicine (P.d.A. ✉ *philippe.dabadie@uclouvain.be*, S.W., A.v.M., R.L., F.J.), Department of Interventional Radiology (P.G., N.A.), Saint Luc University Hospital and King Albert II Cancer Institute, Brussels, Belgium.

Received 1 October 2020; revision requested 23 October 2020; last revision received 10 February 2021; accepted 19 February 2021.

Published online 3 November 2021.

DOI 10.5152/dir.2021.20785

You may cite this article as: d'Abadie P, Walrand S, Goffette P, et al. Antireflux catheter improves tumor targeting in liver radioembolization with resin microspheres. Diagn Interv Radiol 2021; 27:768–773.

(ARC), i.e., Surefire Infusion System® (Surefire Medical Inc.). ARC has a funnel shaped expanding tip designed to minimize reflux of radioactive microspheres and the risk of extrahepatic deposition (6, 7). Changes in the downstream hepatic arterial blood pressure were reported using this catheter (8). When the ARC is deployed, the arterial blood pressure decreases in the antegrade distribution and may reduce the resistance in the tumor vasculature. This hemodynamic effect seems responsible for an increase in tumor targeting in some previous reports (9, 10).

Our study aims to compare tumor to normal liver ratio (T/NL) and tumor absorbed doses (TD) when a conventional end-hole catheter (EHC) and an ARC are used in the same patient at two different time points. As a second endpoint, we investigated this effect as a function of the tumor type.

Methods

Procedures

Patients treated by radioembolization with resin microspheres were retrospectively analyzed from 2010 to 2019 after approval by the local ethics committee (2017/27JUI/334). Informed consent was waived because the entire study was retrospective. Each procedure was performed according to standards of clinical practice (2). A planning angiography was performed to identify the vascular supply of the tumor, to embolize some extrahepatic branches and finally radioembolization was simulated with ^{99m}Tc-MAA injection (TechneScan LyoMAA, Mallinckrodt Medical BV and Curium). Then, ^{99m}Tc-MAA SPECT imaging was obtained to confirm the absence of extrahepatic uptake and allowed to quantify a potential hepatopulmonary shunt. Within 1 to 3 weeks following the planning angiography, ^{90}Y-resin microspheres were injected (activity determined according to the BSA method), and the treatment was followed by a ^{90}Y PET/CT to assess the ^{90}Y microspheres deposition.

Characteristics of each arteriography were reviewed by a senior interventional radiologist and only procedures (planning and therapy) performed with similar catheter tip placement are reported in this study. Angiograms with differences in excess of 2 cm in catheter tip positions were excluded from the analysis. ARC was used for patients with high-risk liver anatomy, particularly for microsphere injection in the close vicinity of a non-embolizable hepato-enteric arterial branch, to avoid extra-hepatic deposition. This decision though was left to the senior interventional radiologist, without randomization. All arteriographies were performed without the use of cone-beam CT.

The preliminary arteriography was always executed with a conventional EHC. Patients treated with use of ARC were classified as the ARC group and the control group was defined as patients in whom EHC was used in both planning and therapeutic arteriographies.

Patients and tumors

Patients and tumor characteristics are summarized in Tables 1 and 2. Briefly, 38 patients with 115 lesions were identified in the ARC group and 23 patients with 75 lesions in the control group. In the ARC group, the types of tumors were colorectal metastases (CRM) with 48 lesions (41.7%), neuroendocrine metastases (NEM) with 30 lesions (26.1%) and HCC with 24 lesions (20.9%), as compared with 22 lesions (29.3%), 34 lesions (45.3%) and 19 lesions (25.3%) in the control group, respectively.

Imaging protocols

^{99}Tc-MAA SPECT/CT was performed within 1 hour after injection of 150 to 170 MBq using a Brightview XCT scanner (Philips Healthcare). Abdominal SPECT images were acquired with a 128×128 matrix with a low energy-high resolution collimator (64 angles per head, 25 s/angle). Image reconstruction was achieved using an OSEM algorithm (8 iterations and 16 subsets) with attenuation and scatter corrections.

^{90}Y post-treatment imaging was performed with a time-of-flight (TOF) PET/CT (Gemini TF, Philips Medical Systems) with an abdominal acquisition of 40 minutes (2 bed positions). Reconstruction was performed with the 3D line of response (LOR)-TOF blob-based algorithm (2 iterations, 33 subsets) and with a voxel reconstruction of 4×4×4 mm^3.

Tumor uptake and tumor absorbed dose

Lesions were first delineated using the baseline contrast-enhanced magnetic resonance imaging or CT scan with MIM 6.7 (MIM Software Inc.) performed before the workup. In 3 patients of the ARC group, tumor delineation was based on fluorodeoxyglucose PET/CT because no baseline MRI or contrast-enhanced CT scan was available before treatment. Volumes of interest (normal liver and tumors) were fused with ^{99}Tc-MAA SPECT and ^{90}Y PET/CT using a rigid co-registration.

Main points

- Compared to classic end-hole catheters, antireflux catheters improve tumor to normal liver uptake ratios and tumor absorbed doses in liver radioembolization.
- This effect was mainly demonstrated for the treatment of neuroendocrine metastases and hepatocellular carcinoma and was minor for colorectal metastases.
- By increasing tumor to normal liver ratio and tumor dose using antireflux catheter, one could expect in future studies, a better clinical response to liver radioembolization which is strongly correlated to high tumor targeting.

Table 1. Patient characteristics

Characteristics		ARC group (n=38)	Control group (n=23)	*p*
Sex, n (%)	Female	11 (28.9)	8 (34.8)	0.633
	Male	27 (71.1)	15 (65.2)	
Age (years)	Median (IQR)	65.5 (17.7)	68.0 (12)	0.421
Tumor type, n (%)	Cholangiocarcinoma	2 (5.3)	0 (0.0)	0.288
	Colorectal	15 (39.5)	6 (26.1)	
	HCC	9 (23.7)	10 (43.5)	
	Melanoma	3 (7.9)	0 (0.0)	
	Neuroendocrine	8 (21.1)	7 (30.4)	
	Esophagus	1 (2.6)	0 (0.0)	
No. of lesions per patient	Median (IQR)	3.0 (2)	2.0 (4)	0.421

ARC, antireflux catheter; IQR, interquartile range; HCC, hepatocellular carcinoma.
For continuous variables, Mann-Whitney U test was used. For categorical variables, comparisons were made using chi-square test or, when expected counts was low, a Fisher-Freeman-Halton test.

Table 2. Individual lesions characteristics

Characteristics		ARC group (n=115)	Control group (n=75)	*p*
Lesion volume (mL)	Median (IQR)	25.3 (73.6)	10.8 (20.5)	0.010*
Target, n (%)	Whole liver (bilobar)	51 (44.3)	46 (61.3)	0.052
	Lobar	58 (50.4)	28 (37.3)	
	Selective	6 (5.2)	1 (1.3)	
Tumor type, n (%)	Colorectal m.	48 (41.7)	22 (29.3)	0.001*
	HCC	24 (20.9)	19 (25.3)	
	Neuroendocrine m.	30 (26.1)	34 (45.3)	
	Miscellaneous	13 (11.3)	0 (0.0)	

ARC, antireflux catheter; IQR, interquartile range; m., metastases; HCC, hepatocellular carcinoma.
For continuous variables, Mann-Whitney U test was used. For categorical variables, comparisons were made using chi-square test or, when expected counts was low, a Fisher-Freeman-Halton test.
*Indicates a significant result at a 5% type I error.

Table 3. Tumor uptake and dose in groups

Groups	Characteristics		MAA	^{90}Y	*p*
ARC n=115	T/NL	Median (IQR)	1.74 (1.43)	2.16 (2.15)	<0.001*
	Dose (Gy)	Median (IQR)	73.72 (62.82)	90.96 (98.31)	<0.001*
Control n=75	T/NL	Median (IQR)	1.60 (2.04)	1.57 (1.38)	0.892
	Dose (Gy)	Median (IQR)	72.92 (80.33)	66.88 (87.71)	0.950

MAA, macroaggregated albumin; ARC, antireflux catheter; IQR, interquartile range; T/NL, tumor to normal liver uptake.
Wilcoxon signed rank test was used for the analysis of patient-paired difference between MAA and ^{90}Y.
*Indicates a significant result at a 5% type I error.

Table 4. Tumor type analysis in the ARC group

Tumor type	Characteristics		MAA	^{90}Y	*p*
Hepatocellular carcinoma n= 24 (20.9%)	T/NL	Median (IQR)	2.06 (2.10)	2.80(1.94)	0.010*
	Dose	Median (IQR)	95.36 (110.79)	135.23 (116.40)	0.034*
Neuroendocrine metastases n= 30 (26.1%)	T/NL	Median (IQR)	1.88 (1.30)	2.97(4.34)	<0.001*
	Dose	Median (IQR)	80.89 (63.52)	125.16 (127.07)	0.009*
Colorectal metastases n=48 (41.7%)	T/NL	Median (IQR)	1.57 (1.01)	1.80(1.18)	0.162
	Dose	Median (IQR)	62.22 (62.93)	70.26 (72.97)	0.039*

ARC, antireflux catheter; MAA, macroaggregated albumin; IQR, interquartile range; T/NL, tumor to normal liver uptake.
Wilcoxon signed rank test was used for the analysis of patient-paired difference between MAA and ^{90}Y.
*Indicates a significant result at a 5% type I error.

The tumor to normal liver uptake ratio (T/NL) is a concentration ratio defined as:

$$T/NL = \frac{Counts_t / Volume_T}{Counts_{NL} / Volume_{NL}}$$

where $Counts_T$ represents the total counts on the entire tumor volume of each individual tumor (diameter superior to 1 cm) and $Counts_{NL}$ the total counts in the injected normal liver volume. $Counts_T$ and $Counts_{NL}$ were measured from ^{99m}Tc-MAA SPECT or ^{90}Y PET/CT datasets.

The absorbed dose to tumors was determined by the simplified MIRD-based equation (11, 12):

$$TD = \frac{Injected\ Activity\ (GBq)\ .50\ .(1\text{-}LSF)\ .f_{(tumor)}}{Tumor\ mass\ (kg)}$$

where *LSF is* the lung shunt fraction and f_{tumor}, the fractional uptake of the tumor defined on ^{99m}Tc-MAA SPECT and on ^{90}Y PET/CT:

$$f_{tumor} = \frac{total\ counts_{tumor}}{total\ counts_{liver}}$$

At the end, for each lesion a set of 4 data was available for analysis: for ^{99m}Tc-MAA SPECT, T/NL_{MAA} and TD_{MAA} and for ^{90}Y PET/CT, T/NL_{90Y} and TD_{90Y}.

Statistical analysis

Analyses were conducted using SAS V9.4 software (SAS Institute Inc.). The main objective was to compare tumor uptake and tumor dose between ^{99m}Tc-MAA SPECT and ^{90}Y PET/CT. T/NL_{MAA} and TD_{MAA} with T/NL_{90Y} and TD_{90Y}, respectively, were compared within each group (ARC and control separately) using a Wilcoxon signed rank test. The homogeneity of the patient and lesion characteristics were compared between the two groups using a Mann-Whitney U test for the continuous variables. For categorical variables, comparisons were made using a chi-square test or, when expected counts problem occurred, a Fisher-Freeman-Halton test. $p < 0.05$ was accepted as the significance level. Descriptive statistics were presented using frequencies with percentages, 95% confidence interval (95% CI) of the medians and interquartile ranges.

Results

When pooling all tumors from both groups, where all patients received the ^{99m}Tc-MAA injection using EHC, the median T/NL_{MAA} was 2.19 in HCC (95% CI, 1.53–2.85), 1.82 in NEM (95% CI 1.57–2.43) and 1.35 for CRM (95% CI, 1.16–1.68). T/NL_{MAA} was significantly lower in CRM compared to NEM ($p = 0.010$) and HCC ($p = 0.002$).

In the ARC group, T/NL_{90Y} and TD_{90Y} were significantly higher than T/NL_{MAA} and TD_{MAA} (Fig. 1 left panel; Tables 3 and 4). Detailed data per individual tumor type are given in Table 4. The tumor dose was significantly increased by a median 23% between the planning (measured using ^{99}Tc-MAA SPECT/CT, EHC used) and the treatment (measured using the ^{90}Y PET/CT, ARC used). The increase of TD was the highest in NEM (increase of 55% between medians; $p = 0.009$), followed by HCC (increase of 42% between medians; $p = 0.034$), and lowest for CRC (increase of 13% between medians; $p = 0.039$), as demonstrated in Table 4 (example of a NEM patient in Fig. 2). Similarly, T/NL was also increased by a median of 24% over the entire population of ARC patients ($p < 0.001$), with an increment of 36% in HCC ($p = 0.010$), 58% in NEM ($p < 0.001$) and only 15% in CRC patients ($p = 0.162$, not significant).

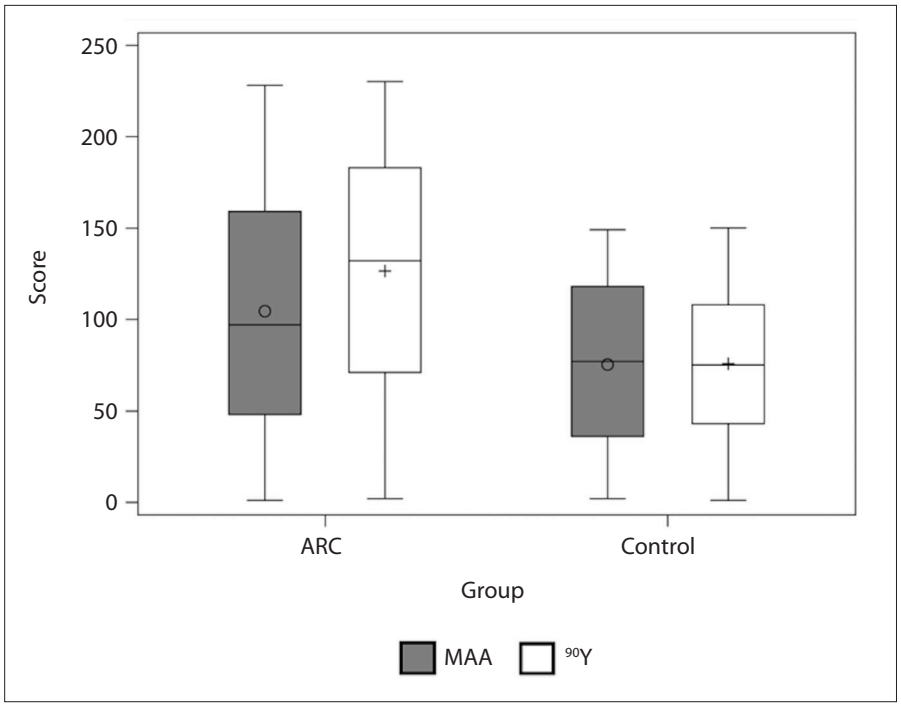

Figure 1. Signed rank scores for tumor to normal liver uptake ratio (T/NL) observed with ^{99m}Tc-MAA SPECT/CT (MAA) and ^{90}Y PET/CT (90Y) in the ARC group (left) and in the control group (right).

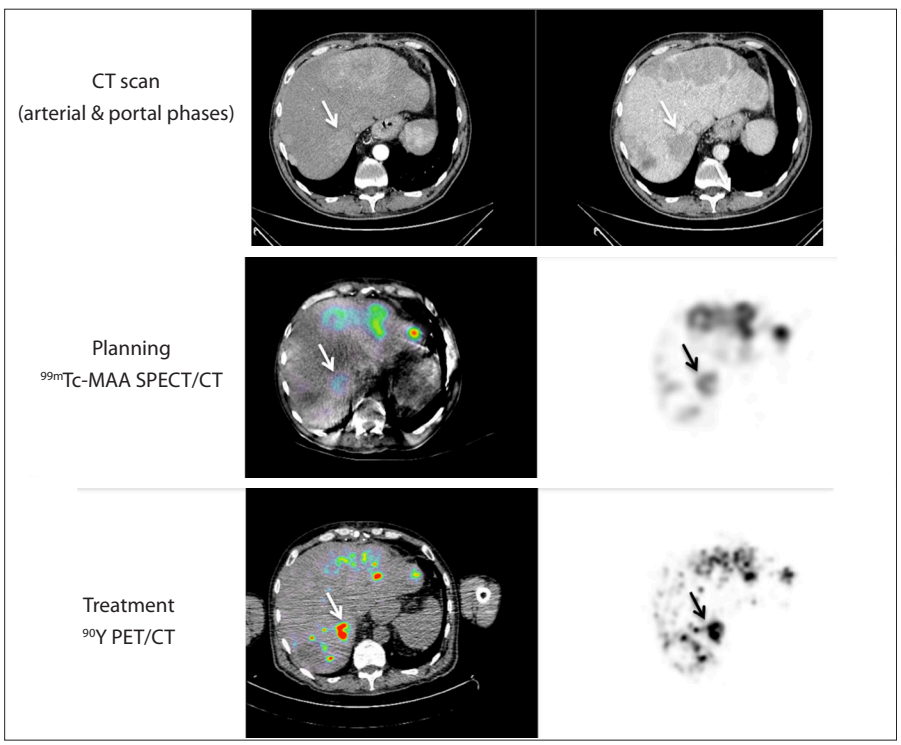

Figure 2. Example of a patient treated by liver radioembolization for high hypervascular neuroendocrine metastases demonstrated on CT scan (upper panel). The planning (middle panel) was performed with a classic end-hole catheter; T/NL and tumor dose were respectively 2.9 and 69 Gy in the tumor located in segment 7 *(arrow)*. The treatment (lower panel) was performed with an antireflux catheter; T/NL and tumor dose were respectively 8.4 and 172 Gy in this same tumor *(arrow)*.

In the control group, no statistically significant difference was observed for neither the T/NL nor the TD between the planning and the post-treatment study (Fig. 1 right panel; Table 3). In addition, no significant difference in tumor uptake (T/NL) was observed for any tumor type (data not shown).

Discussion

Our study demonstrates that, using an ARC, an improvement of the T/NL of 36%, 58%, and 15% is obtained in HCC, NEM, and CRM, respectively (Table 4). In all radiation therapy applications, improving the absorbed dose to tumors, without increasing the dose to non-target tissues (which is expressed by the T/NL ratio), is a goal that cannot be overlooked. Better tumor targeting leads to higher doses to tumors and a higher probability of tumor control (1). Furthermore, the tumor control probability (TCP) as a function of the dose has a sigmoid shape (5, 13), resulting in the fact that little increases or decreases of tumor doses, close to the therapeutic window, may result in a major effect on clinical response or progression, respectively. Besides these scientific considerations, international authorities (e.g., Euratom 2013/59 and ICRP 140) strongly encourage all efforts towards dose optimization (14, 15).

Interestingly, a recent secondary analysis of the SARAH prospective study demonstrated a significant improvement in disease control and overall survival in radioembolization of HCC with a tumor dose above 100 Gy (16). Very recently, another study demonstrated that adding pre-therapeutic dosimetry as a tool for optimization results in better outcome (17).

Why ARC improves tumor targeting is not totally understood. The downstream blood flow distribution is modified when the catheter tip is deployed. The occlusion level of this tip is dynamic, occlusive during the diastole. Similarly, if a retrograde flow appears, the expandable tip stays open and precludes reflux. A study by Rose et al. (8) demonstrated a significant decrease of the blood pressure in the downstream arterial compartment. To maintain an antegrade flow in the downstream compartment, the pressure in the downstream vascular bed must be lower than the pressure near the catheter tip. Resistance in the downstream compartment may decline more and more distally by opening or recruiting new arteries. Arepally et al. (7) illustrate this effect in an *ex vivo* study: in a swine model, the penetration of tantalum microspheres in the renal parenchyma was deeper with an ARC as compared with standard catheters. The microsphere distribution was visually more

homogeneous and more extended to distal vessels (7). The distal pressure reduction induced by the deployment of this expandable tip is similar to what is demonstrated with the use of a microballoon catheter in transarterial chemoembolization (18). Pasciak et al. (10) proposed another interpretation: the reduction of the downstream pressure may be induced by vasoconstriction of normal liver arteries, delivering more microspheres to tumor arteries (10). Moreover, in contrast with a conventional catheter, ARC allows an optimized centering of the catheter tip in the vessel lumen and generates a turbulent-like flow during the microsphere administration (19, 20). These effects are responsible for a more homogeneous distribution in the downstream network. With a computer model of the hepatic artery and tumor vessels, Kennedy et al. (21) demonstrated an increase in the tumor microsphere deposition when the flow was homogeneous.

Our study confirms some previous data. In a small prospective trial (n=9), Pasciak et al. (10) performed for each patient two procedures of lobar infusions of ^{99}Tc-MAA in a nonrandomized 2 by 2 crossover design one-day protocol (10). One infusion was performed with an ARC and the other with an EHC. Tumor deposition increased between 33.0% to 90.0% with the ARC. In this study, lesions were mostly HCC (n=6). In a controlled trial conducted with 25 patients treated for CRM with holmium-166 (^{166}Ho) microspheres, the ARC was randomly allocated to the left or right liver artery and the standard catheter to the contralateral artery (9). The mean T/NL ratio was increased by 25.0% when lesions were treated using an ARC.

The current study also highlights other findings. In the ARC group, increases in tumor uptake and tumor dose between the planning arteriography (with an EHC) and the treatment arteriography (with an ARC) were variable according to the tumor type: highly significant for NEM and HCC, modest for CRM. These differences could be explained by changes in tumor perfusion. Indeed, tumor targeting in ^{90}Y radioembolization depends on tumor arterial vascularization because microspheres are deposited preferentially in the terminal arterioles. NEM are often hypervascular with higher enhancement during a dynamic enhanced-contrast CT scan compared to other types of metastases (22). On the contrary, CRM are often less perfused (23). Moreover, tumor arterial perfusion assessed by ^{99m}Tc MAA SPECT/CT confirmed in our study a higher tumor uptake for NEM and HCC as compared to CRM.

Our study has some limitations. First, although it is an intra-patient comparison, our analysis is based on a comparison between two different radiolabeled vectors (^{99m}Tc-MAA and ^{90}Y microspheres) and the assumption of a good correlation between their respective behaviors. This consideration is questionable mainly due to physical differences between ^{99}Tc-MAA particles and ^{90}Y-microspheres, including differences in size, number, density and amount of radioactivity per particle (24). A good reproducibility between ^{99m}Tc-MAA and ^{90}Y-microspheres requires also similar angiographic conditions and especially similar catheter positions (3). Minor differences in catheter tip positions could induce important differences in particle distributions (25, 26). With regards to ^{90}Y PET/CT, previous studies confirmed a good accuracy of the technique to assess tumor uptake and absorbed doses after ^{90}Y-radioembolization (27, 28). Some previous studies also demonstrated a good correlation between ^{99m}Tc-MAA SPECT and ^{90}Y PET/CT dosimetry (29–32). However, the reproducibility of dosimetry based on ^{99m}Tc-MAA SPECT/CT as compared with the ^{90}Y PET/CT is not fully established and individual variations in tumor dose estimation can occur. To cope with this problem, we introduced a control group where ^{99m}Tc-MAA and ^{90}Y microspheres injections were performed with the same type of microcatheter. This group confirmed that there were no significant differences between ^{99m}Tc-MAA and ^{90}Y microspheres in tumor deposition. Second, this study is retrospective and the use of the ARC instead of a standard microcatheter was not randomized but left to the decision of the interventional radiologist. In the future, controlled prospective trials are needed to investigate the effect of ARC in tumor response and survival after ^{90}Y radioembolization. Moreover, the changes in tumor targeting using ARC are not clearly understood and require more experiments with fluid particle models, using either *ex vivo* or mathematical models.

In conclusion, our results support the use of ARC to improve tumor targeting in ^{90}Y radioembolization using resin microspheres. ARC impacts the risk-benefit ratio during a procedure of ^{90}Y microspheres infusion, by decreasing the risk of extrahepatic deposition as previously known, but also by improving the targeting efficiency. Also, as shown by Morshedi et al. (33), ARC is a cost-effective alternative to standard end-hole catheter, reducing the time of the procedure and the use of coil-embolization.

Acknowledgements

We are very grateful to Aline Van Maanen and Kiswendsida Sawadogo from the Department of Biostatistics (Saint Luc University hospital and King Albert II cancer Institute) for the statistical analysis.

Conflict of interest disclosure

The authors declared no conflicts of interest.

References

1. Cremonesi M, Chiesa C, Strigari L, et al. Radioembolization of hepatic lesions from a radiobiology and dosimetric perspective. Front Oncol 2014; 4:210. [Crossref]
2. Padia SA, Lewandowski RJ, Johnson GE, et al. Radioembolization of hepatic malignancies: background, quality improvement guidelines, and future directions. J Vasc Interv Radiol 2017; 28:1–15. [Crossref]
3. Garin E, Rolland Y, Laffont S, et al. Clinical impact of (99m)Tc-MAA SPECT/CT-based dosimetry in the radioembolization of liver malignancies with (90)Y-loaded microspheres. Eur J Nucl Med Mol Imaging 2016; 43:559–575. [Crossref]
4. Ho S, Lau WY, Leung TW, et al. Partition model for estimating radiation doses from yttrium-90 microspheres in treating hepatic tumours. Eur J Nucl Med 1996; 23:947–952. [Crossref]
5. Strigari L, Sciuto R, Rea S, et al. Efficacy and toxicity related to treatment of hepatocellular carcinoma with 90Y-SIR spheres: radiobiologic considerations. J Nucl Med 2010; 51:1377–1385. [Crossref]
6. Van den Hoven AF, Prince JF, Samim M, et al. Posttreatment PET-CT-confirmed intrahepatic radioembolization performed without coil embolization, by using the antireflux Surefire Infusion System. Cardiovasc Intervent Radiol 2014; 37:523–528. [Crossref]
7. Arepally A, Chomas J, Kraitchman D, et al. Quantification and reduction of reflux during embolotherapy using an antireflux catheter and tantalum microspheres: ex vivo analysis. J Vasc Interv Radiol 2013; 24:575–580. [Crossref]
8. Rose SC, Kikolski SG, Chomas JE. Downstream hepatic arterial blood pressure changes caused by deployment of the surefire antireflux expandable tip. Cardiovasc Intervent Radiol 2013; 36:1262–1269. [Crossref]
9. Van den Hoven AF, Prince JF, Bruijnen RC, et al. Surefire infusion system versus standard microcatheter use during holmium-166 radioembolization: study protocol for a randomized controlled trial. Trials 2016; 17:520. [Crossref]
10. Pasciak AS, McElmurray JH, Bourgeois AC, Heidel RE, Bradley YC. The impact of an antireflux catheter on target volume particulate distribution in liver-directed embolotherapy: a pilot study. J Vasc Interv Radiol 2015; 26:660–669. [Crossref]

11. Giammarile F, Bodei L, Chiesa C, et al. EANM procedure guideline for the treatment of liver cancer and liver metastases with intra-arterial radioactive compounds. Eur J Nucl Med Mol Imaging 2011; 38:1393–1406. [Crossref]
12. Spahr N, Schilling P, Thoduka S, Abolmaali N, Schenk A. Predictive SIRT dosimetry based on a territorial model. EJNMMI Phys 2017; 4:25. [Crossref]
13. Dewaraja YK, Devasia T, Kaza RK, et al. Prediction of tumor control in (90)Y radioembolization by logit models with PET/CT-based dose metrics. J Nucl Med 2020; 61:104–111. [Crossref]
14. Council Diective 2013/59/Euratom. Basic safety standards for protection against the dangers arising from exposure to ionising radiation, and repealing directives 89/618/Euratom, 90/641/Euratom, 96/29/Euratom, 97/43/Euratom and 2003/122/Euratom.
15. ICRP. Radiological protection in therapy wuth radiopharmaceuticals. Ann ICRP 48. 2019; Publication 140. [Crossref]
16. Hermann AL, Dieudonne A, Ronot M, et al. Relationship of tumor radiation-absorbed dose to survival and response in hepatocellular carcinoma treated with transarterial radioembolization with (90)Y in the SARAH Study. Radiology 2020; 296:673–684. [Crossref]
17. Garin E, Tselikas L, Guiu B, et al. Personalised versus standard dosimetry approach of selective internal radiation therapy in patients with locally advanced hepatocellular carcinoma (DOSISPHERE-01): a randomised, multicentre, open-label phase 2 trial. Lancet Gastroenterol Hepatol 2021; 6:17–29. [Crossref]
18. Irie T, Kuramochi M, Takahashi N. Dense accumulation of lipiodol emulsion in hepatocellular carcinoma nodule during selective balloon-occluded transarterial chemoembolization: measurement of balloon-occluded arterial stump pressure. Cardiovasc Intervent Radiol 2013; 36:706–713. [Crossref]
19. Van den Hoven AF, Lam MG, Jernigan S, van den Bosch MA, Buckner GD. Innovation in catheter design for intra-arterial liver cancer treatments results in favorable particle-fluid dynamics. J Exp Clin Cancer Res 2015; 34:74. [Crossref]
20. Aramburu J, Anton R, Rivas A, Ramos JC, Sangro B, Bilbao JI. Computational assessment of the effects of the catheter type on particle-hemodynamics during liver radioembolization. J Biomech 2016; 49:3705–3713. [Crossref]
21. Kennedy AS, Kleinstreuer C, Basciano CA, Dezarn WA. Computer modeling of yttrium-90-microsphere transport in the hepatic arterial tree to improve clinical outcomes. Int J Radiat Oncol Biol Phys 2010; 76:631–637. [Crossref]
22. Namasivayam S, Martin DR, Saini S. Imaging of liver metastases: MRI. Cancer Imaging 2007; 7:2–9. [Crossref]
23. Schima W, Kulinna C, Langenberger H, Ba-Ssalamah A. Liver metastases of colorectal cancer: US, CT or MR? Cancer Imaging 2005; 5 Spec No A:S149–156. [Crossref]
24. Van de Wiele C, Maes A, Brugman E, et al. SIRT of liver metastases: physiological and pathophysiological considerations. Eur J Nucl Med Mol Imaging 2012; 39:1646–1655. [Crossref]
25. Aramburu J, Anton R, Rivas A, Ramos JC, Sangro B, Bilbao JI. Computational particle-haemodynamics analysis of liver radioembolization pretreatment as an actual treatment surrogate. Int J Numer Method Biomed Eng 2017; 33. [Crossref]
26. Aramburu J, Anton R, Rivas A, Ramos JC, Sangro B, Bilbao JI. Liver radioembolization: an analysis of parameters that influence the catheter-based particle-delivery via CFD. Curr Med Chem 2020; 27:1600–1615. [Crossref]
27. Lhommel R, Van Elmbt L, Goffette P, et al. Feasibility of 90Y TOF PET-based dosimetry in liver metastasis therapy using SIR-Spheres. Eur J Nucl Med Mol Imaging 2010; 37:1654–1662. [Crossref]
28. Gates VL, Esmail AA, Marshall K, Spies S, Salem R. Internal pair production of 90Y permits hepatic localization of microspheres using routine PET: proof of concept. J Nucl Med 2011; 52:72–76. [Crossref]
29. Jadoul A, Bernard C, Lovinfosse P, et al. Comparative dosimetry between (99m)Tc-MAA SPECT/CT and (90)Y PET/CT in primary and metastatic liver tumors. Eur J Nucl Med Mol Imaging 2019; 47:828–837. [Crossref]
30. Gnesin S, Canetti L, Adib S, et al. Partition model-based 99mTc-MAA SPECT/CT predictive dosimetry compared with 90Y TOF PET/CT posttreatment dosimetry in radioembolization of hepatocellular carcinoma: a quantitative agreement comparison. J Nucl Med 2016; 57:1672–1678. [Crossref]
31. Knesaurek K, Tuli A, Pasik SD, Heiba S, Kostakoglu L. Quantitative comparison of pre-therapy (99m)Tc-macroaggregated albumin SPECT/CT and post-therapy PET/MR studies of patients who have received intra-arterial radioembolization therapy with (90)Y microspheres. Eur J Radiol 2018; 109:57–61. [Crossref]
32. Kafrouni M, Allimant C, Fourcade M, et al. Analysis of differences between (99m)Tc-MAA SPECT- and (90)Y-microsphere PET-based dosimetry for hepatocellular carcinoma selective internal radiation therapy. EJNMMI Res 2019; 9:62. [Crossref]
33. Morshedi MM, Bauman M, Rose SC, et al. Yttrium-90 resin microsphere radioembolization using an antireflux catheter: an alternative to traditional coil embolization for nontarget protection. Cardiovasc Intervent Radiol 2015; 38:381–8. [Crossref]